Robust LiDAR-Based Parking Slot Detection and Pose Estimation for Shell Eco-Marathon Vehicles

Miklós Unger[a] and Ernő Horváth[b]
Research Center of Vehicle Industry, Széchenyi István University, 1 Egyetem Square, Győr, Hungary

Keywords: Autonomous Vehicles, Shell Eco-Marathon, Parking Place Detection, LIDAR.

Abstract: This paper introduces the winning algorithm of the 2024 Shell Eco-marathon Autonomous Urban Challenge for autonomous parking. The task requires the vehicle to identify an available parking spot from multiple alternatives and precisely navigate into it, fully remaining within the designated area without touching any lane markings. Successful task execution requires not only reliable long-range detection of the parking space but also an accurate final orientation relative to the parking spot. To solve this task, we propose a novel method which relies on the combination neural networks and traditional point cloud processing methods. Since this is a highly specific problem tailored to the Shell Eco-marathon setting, and no publicly available solutions from other teams have been observed, our earlier algorithm serves as the primary baseline for comparison.

1 INTRODUCTION

The Shell Eco-marathon is an international university competition that promotes the design of energy-efficient vehicles and includes autonomous driving challenges. In the autonomous category, participants must complete three main tasks without any external intervention: autonomous driving, obstacle avoidance, and parking. SZEnergy Team is a student team participating in this competition. The team's vehicle is equipped with a 128-channel Ouster LiDAR, a ZED2i stereo camera, and an inertial measurement unit (IMU) to support autonomous functionality. The algorithms run on an NVIDIA Jetson Orin onboard computer, using the ROS 2 framework.

1.1 The Race

The competition consists of three main autonomous tasks, with the third and final one being autonomous parking. Between each task, the vehicle is required to come to a complete stop at designated stop lines with stop signs. The competition is typically held on a closed racing circuit; in 2025, it took place at the Silesia Ring in Poland.

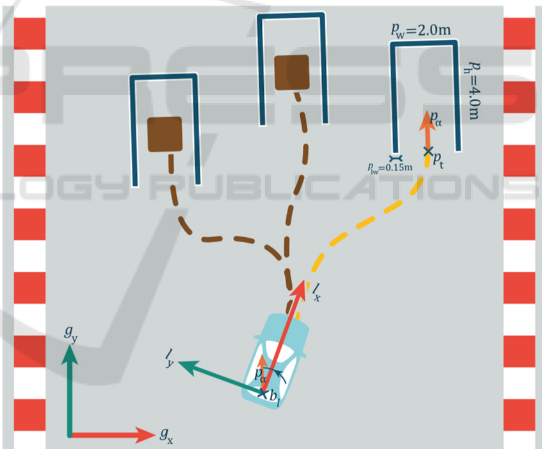

Figure 1: Conceptual Overview of the Challenge.

Due to the layout of the track, the distance between the last stop sign and the parking area can be as much as 50–80 meters. This means that the available parking spot may not be visible immediately, even to the onboard camera. In the parking challenge, three parking spots are placed on different parts of the track using adhesive markings, with two of them intentionally made unavailable. The core challenge

[a] https://orcid.org/0000-0003-3518-1107
[b] https://orcid.org/0000-0001-5083-2073

Unger, M. and Horváth, E.
Robust LiDAR-Based Parking Slot Detection and Pose Estimation for Shell Eco-Marathon Vehicles.
DOI: 10.5220/0013772900003982

In *Proceedings of the 22nd International Conference on Informatics in Control, Automation and Robotics (ICINCO 2025) - Volume 1*, pages 486-493
ISBN: 978-989-758-770-2; ISSN: 2184-2809

for the algorithm is to reliably detect and select the one unoccupied parking spot, see figure 1 and 2.

Figure 1 illustrates an autonomous vehicle maneuvering through a parking challenge consisting of multiple slots. Each parking slot is framed by 0.15-meter-wide blue lines with white borders (p_{lw}) along the sides and the back, defining a 2.0-meter-wide (p_w) and 4.0-meter-deep (p_h) rectangular parking area. The parking goal position is represented by the point pt, and its desired orientation is indicated by the vector p_α (marked with an orange arrow and displayed two times for clarity). An example trajectory to a free parking space is shown with a dashed yellow curve, while trajectory to an occupied parking space is marked with brown dashed curves.

The vehicle is equipped with a body-fixed local coordinate system, denoted as (l_x, l_y), while the global frame is labelled (g_x, g_y). Accurate alignment with the target pose pα is critical for successful parking. The b_l refers to the base_link frame, and the variable distance represents the Euclidean distance between b_l and the point p_t.

Figure 2: actual picture of the challenge.

2 THE ALGORITHM

The algorithm operates as follows. First, a trained neural network identifies a bounding box in the image data, which it predicts—based on a certain confidence value—to represent a free parking space. The algorithm is designed in such a way that, even if multiple parking spaces are detected, it only publishes the corner points of the bounding box with the highest confidence on a ROS topic. This information is then used for further processing.

Initially, these four corner points are only available as 2D pixel coordinates. Through a deprojection process, the algorithm converts them into 3D coordinates and then transform them into the appropriate reference frame using the corresponding transforms.

Until reliable LiDAR data becomes available—as described in the following sections—The car initiate motion towards the estimated center of the parking slot based solely on the bounding box identified in the camera image.

After the corner points are transformed into the appropriate reference frame, the LiDAR point cloud is analysed within the defined region. Specifically, the algorithm focuses on the ambient and intensity values associated with the points. Based on the observations, there is a significant difference in ambient response between bare asphalt/concrete and painted surfaces, with the latter typically producing sharp peaks in the ambient signal (Jing Gong et al.,2024).

Our objective is to identify which points in the cloud correspond to the painted parking area. In earlier versions of the software, this was attempted by comparing each point's ambient value to a global average. In the current approach, however, the algorithm relies solely on detecting significant peaks in ambient values, as they have proven to be a more reliable indicator of painted regions.

In the context of parking spot detection and the actual parking maneuver, our algorithmic objective is to generate a pose-type ROS topic. The position component of this pose is defined such that its lateral coordinate aligns with the center of the parking spot, while its longitudinal coordinate is aligned with the starting edge of the painted boundary lines. This position can optionally be adjusted in the longitudinal direction depending on how deep the vehicle is intended to enter the parking space (Weikang et al.,2024).

The more critical aspect, however, is the orientation of this pose. It is essential that the vehicle aligns itself straight within the parking area, avoiding any skewed positioning. This requirement arises because the camera-based parking space detector only returns a 2D bounding box with width and height, but without any reliable orientation information. Therefore, the detection is augmented with LiDAR-based analysis to derive a pose that includes an accurate angular alignment relative to the actual orientation of the painted parking lines (Hata and Wolt, 2014)

The construction of the final pose proceeds as follows: within the filtered bounding box, the LiDAR point cloud is traversed ring by ring (i.e., by increasing radial distance), and points exhibiting a significant ambient value peak are collected. Ideally, four such points can be detected per ring. Pairs of points lying within 15 cm of each other — a threshold chosen based on the official width specification of the painted parking lines in the competition rulebook — are then clustered.

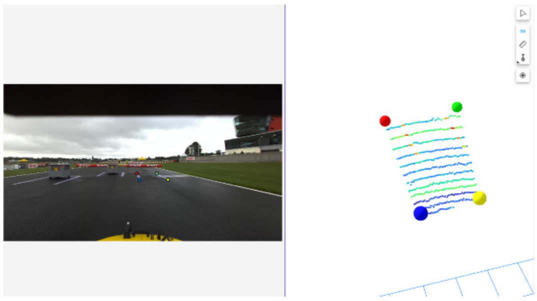

Figure 3: The original pointcloud in the deprojected area. The points in the left represent the same points in the right

The purpose of this clustering is to compute a representative midpoint between the two edge markings of the parking spot These midpoints serve as the basis for determining the centerline of the parking space, from which the desired pose position and orientation are derived for accurate parking alignment (Figure 5).

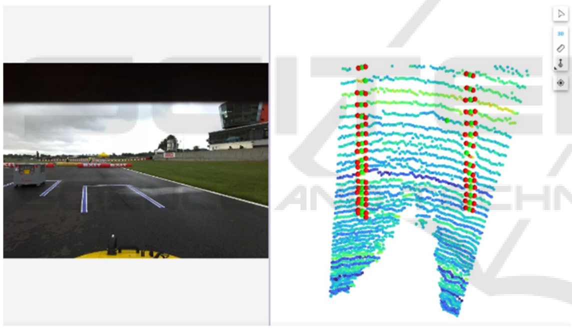

Figure 4: The red dots represent the points where are the ambient value peaks are. The green dots represent the uncategorized points.

Once the points corresponding to the painted line segments — hereafter referred to as uncategorized parking points (The green dots on Figure 4) — are obtained, the next step is to determine whether each point belongs to the left or right side of the parking space.

Initially, the two points closest to the bottom edge of the bounding box are identified. The point located nearer to the lower-left corner is designated as the front-left point, while the other is assigned as the front-right point.

As the vehicle approaches the parking space, additional uncategorized parking points are detected. These are incrementally classified as either left- or right-side points based on their relative position and orientation with respect to the initial front-left and front-right references. Once at least two points have been classified on each side, an average directional orientation is computed per side. New points are subsequently assigned by comparing their local orientation to the corresponding side's average.

To minimize false detections and prevent misclassification due to lateral noise or ambiguity, a strict angular threshold is enforced, allowing a new point to be associated with a side only if its orientation deviates minimally from the corresponding average direction.

In addition to positional and orientational criteria, a lateral distance constraint is also incorporated when classifying points to the left or right side of the parking space. According to the Shell Eco-marathon rulebook, the width of a parking space (p_w). is specified in 2.0 meters. Therefore, during side classification, it is verified that the distance between a newly detected point and the corresponding point on the opposite side falls within this acceptable range. To account for potential sensor noise and minor deviations in perception, a tolerance margin is introduced. If a candidate point lies closer than 1.8 m or farther than 2.1 m from any point already assigned to the opposite side, it is rejected as likely noise or not part of the actual painted boundary (Smith and Müller, 2023).

The final pose estimation is performed once a sufficient number of reliable points have been classified on both sides of the parking space.

At this stage, two lines are constructed based on the initial points from the left and right boundaries, using the respective local orientation estimates. These lines model the painted borders of the parking slot.

The lateral (cross-track) position is computed as the midpoint between the two lines, effectively aligning the pose with the centerline of the parking space.

The longitudinal position is derived from the positions of the front-left and front-right points, which typically mark the entrance of the parking space.

The orientation of the final pose is determined by averaging the orientations of the left and right sides, ensuring the vehicle aligns parallel to the painted boundaries and does not park at an angle (Figure 5).

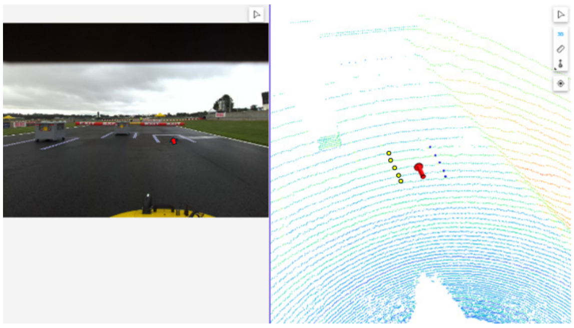

Figure 5: This figure shows the result of our algorithm. The yellow and blue dots represent the two sides of the parking place, the red arrow is our goal pose.

2.1 3D Point Deprojection

To transform 2D image coordinates into 3D camera-space coordinates, a standard deprojection process based on the pinhole camera model is applied. Given a pixel location (u,v) and its corresponding depth value Z (measured along the optical axis), the 3D point (X,Y,Z) in the camera coordinate frame can be computed using the camera's intrinsic parameters as follows:

$$X = \frac{(u - c_x) * Z}{f_x} \quad (1)$$

$$Y = \frac{(v - c_y) * Z}{f_y} \quad (2)$$

$$Z = Z \quad (3)$$

Here, f_x and f_y represent the focal lengths in pixels along the horizontal and vertical axes, respectively, while c_x and f_x denote the optical center (principal point) of the image. These parameters are typically obtained from the camera's intrinsic calibration matrix (K):

$$K = \begin{bmatrix} f_x & 0 & c_x \\ 0 & f_y & c_y \\ 0 & 0 & 1 \end{bmatrix} \quad (4)$$

This computation yields a 3D point in the camera coordinate frame. To express this point in another reference frame - fixed local (l_x, l_y) or global coordinate system (g_x, g_y) - an additional rigid-body transformation must be applied using the appropriate extrinsic parameters (rotation and translation) (Zhang, 2000).

2.2 Results

Before diving into the evaluation results, we first define the three key questions this study aimed to address:

- How does our algorithm perform under different weather conditions? Specifically, can we develop a method that remains robust and functional in both ideal and adverse environmental scenarios, such as rain?
- Can the new method effectively filter outliers, thereby improving the robustness of the estimated pose orientation? Although this paper does not provide an in-depth analysis of pose position accuracy, we aim to indirectly enhance positional robustness by improving orientation stability.
- To what extent does the new method impact the difficulty of detecting parking slots? In other words, does the added complexity of outlier filtering and LiDAR-based refinement compromise the system's responsiveness or detection range?

The comparison of the algorithms is presented through two separate scenarios using two different log files.

While the measurement conditions varied in terms of location and weather, the hardware setup of the vehicle remained identical. From a software perspective, there is no difference in the input data between the two versions.

There is a measurement where two parking spots are available and the left one is free, under sunny and ideal weather conditions and There is the second case where there are three parking spots, with the right one being free, under rainy weather conditions.

One of the key evaluation criteria for the proposed method is its performance under varying environmental conditions, particularly in comparison to our previous parking slot detection approach. A primary metric is the distance from which the first valid points—belonging to either the left or right painted boundary of the parking slot—can be reliably detected, as well as the distance from which a full pose can be estimated.

In rainy conditions, the new method was able to detect valid feature points on both sides of the parking slot from a distance of approximately 15 meters and successfully estimate a reliable pose at 11.4 meters from the parking slot's entrance edge. In contrast, the previous algorithm failed to detect painted boundary features reliably under such weather conditions.

Under clear and sunny weather, the new algorithm detected the parking slot boundaries at approximately 13 meters and computed the pose at approximately 11 meters, maintaining consistent performance. All distance measurements are referenced relative to the leading edge of the parking slot.

Another key aspect of the evaluation is the consistency of the estimated orientation during the entire detection process. Figure 6 shows the absolute orientation values of the generated poses throughout a representative trial compared with the ground truth value. The red dotted line marks the point where the source of orientation data changes: the first 39 outputs are generated by a neural network using the camera image, and all data points after that are provided by the LiDAR-based detection algorithm. show that the output of our algorithm deviates from the ground truth by a maximum of ±0.05 radians (approximately ±2.8 degrees).

During the entire measurement, the vehicle followed a trajectory as illustrated in Figure 1, gradually approaching the pt point

Across the full measurement sequence, the orientation values remained centered around the correct alignment, without significant drift or sudden fluctuations. This level of consistency is essential for ensuring that the vehicle aligns itself correctly within the parking slot and avoids skewed or off-angle final positioning (Figure 6).

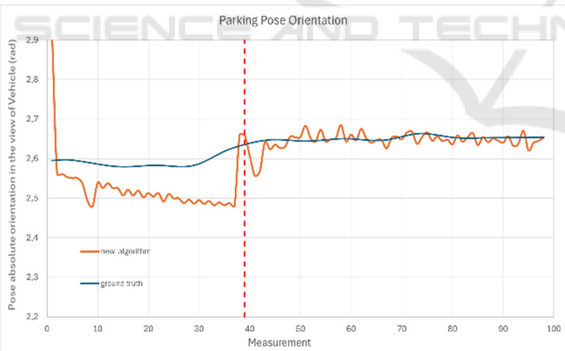

Figure 6: The figure illustrates the pose orientation output by the algorithm as a function of each measurement (X-axis count), expressed in radians. The estimated orientations are compared to the ground truth to evaluate the algorithm's accuracy. The plot includes both the predictions made by the neural network without LiDAR input and those refined using the LiDAR point cloud. The section to the right of the red dashed line marks the point at which orientation estimation begins to incorporate LiDAR data.

It is important to note that the measurements were taken on wet asphalt, where the original version of the algorithm—relying solely on camera input—did not switch to the LiDAR-based method. As a result, this particular sequence is not included in the diagram.

When comparing the results with the previous version of the algorithm—where the main difference lies in the method used to identify the uncategorized parking points—a significant improvement is observed. In the earlier implementation, the filtered point cloud obtained through deprojection was analysed by calculating an average ambient value. Points presumed to belong to the painted lines of the parking space were identified by applying a fixed threshold based on deviation from this average.

However, when analysing the same log file, our previous method failed to detect the parking space under rainy conditions using the LiDAR. As a result, the vehicle relied solely on the camera-based bounding box detection for parking. While the final pose estimation was still positionally acceptable, the orientation did not fully satisfy the competition requirements, highlighting the limitations of the prior approach in low-visibility scenarios (Bézi, 2023).

Under sunny weather conditions, the previous method was able to detect the first points belonging to the painted markings of the parking space from a greater distance—approximately 18 meters. However, due to the absence of orientation constraints during the classification of uncategorized parking points into left and right categories, the older algorithm tended to include several outliers as valid points. These misclassifications directly impacted the stability and accuracy of the estimated orientation, leading to inconsistent pose definitions despite the early detection advantage.

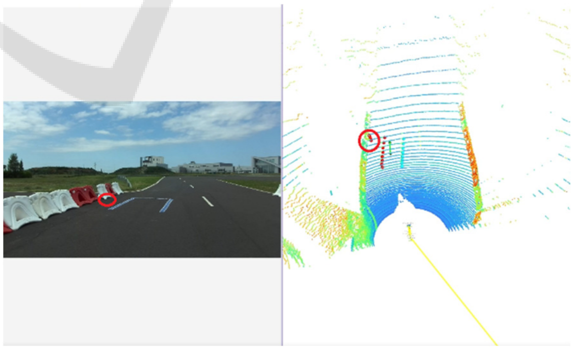

Figure 7: Several points from the water-filled barrier were incorrectly categorized among the left-side points of the parking space.

Figure 8 presents a comparison between the orientation values estimated by the new and the previous algorithms, evaluated against ground truth in a measurement when both algorithms worked correctly. The ground truth reference was established through manual measurements at 25 key points using visual aids to define the expected orientation curve.

The plot also includes orientation values derived from the camera image; thus, during the initial ~50 frames, both algorithms output the same orientation. As the vehicle progresses (after the red dotted line) however, the orientation estimated by the new algorithm remains significantly closer to the ground truth. Most notably, the final orientation computed by the new algorithm deviates by only 0.01 radians (≈ 0.57°) from the ground truth.

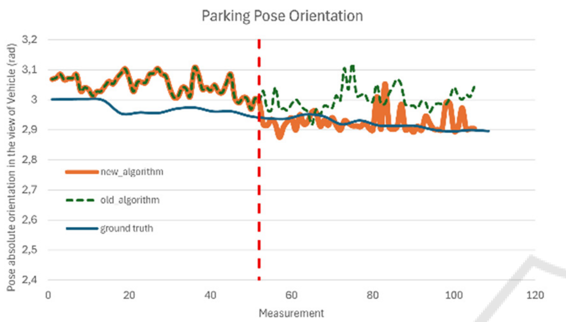

Figure 8: Pose orientation comparison on a dry surface, where both the original and the improved algorithms were active. Similar to Figure 6, this measurement includes the entire dataset, which explains why the outputs of the old and new algorithms are identical before the red dashed line. In this section, both methods relied solely on camera image information for orientation estimation.

2.3 Key Findings

Based on the previous comparison between the two algorithms, the following conclusions can be drawn:

- The previous algorithm is capable of detecting points from one or both sides of the parking slot from a slightly greater distance.
- However, it is more prone to picking up noise, which leads to inaccurate orientation estimation.
- It also struggles to maintain a consistent and precise position throughout the maneuver.
- The previous algorithm did not provide usable results under rainy conditions.

3 CONCLUSIONS

In this work, we have presented a LiDAR-based algorithm developed for autonomous parking within the highly constrained and competitive environment of the Shell Eco-marathon Autonomous Urban Challenge. The method combines neural network-based camera detection with a robust LiDAR point cloud analysis pipeline to derive reliable pose estimates for precise vehicle alignment within painted parking slots.

Our comparative evaluation against a previous algorithm revealed several key findings. While the earlier solution showed some advantages in early detection range under ideal weather conditions—being able to identify features from up to 18 meters away—its lack of strong orientation constraints and susceptibility to noise significantly impacted its accuracy. This often resulted in unstable pose estimates, particularly in the presence of nearby environmental features such as reflective barriers or rain-induced artifacts. Additionally, the prior method failed to provide meaningful output under rainy conditions, a critical limitation in real-world scenarios.

The new algorithm, in contrast, demonstrated a high level of robustness across varying environmental conditions. Even in challenging rainy weather, it successfully detected the key features of the parking slot and generated a stable and accurate pose estimate from more than 11 meters away. One of the most notable advantages is the orientation stability achieved through the improved classification and clustering process. By using ambient signal peaks and carefully calibrated geometric thresholds, the new system achieved an estimated orientation that deviated by no more than ±0.05 radians (≈ ±2.8°) from the ground truth throughout the entire maneuver—demonstrating consistent and accurate alignment. Moreover, the final orientation deviated by as little as 0.01 radians from the ground truth, demonstrating near-perfect alignment with the intended pose.

The practical impact of these improvements is reflected in the SZEnergy Team's successful execution of the parking challenge, which played a decisive role in securing the overall victory in the 2024 Shell Eco-marathon competition. This validates not only the effectiveness of the proposed algorithm but also its ability to operate reliably in real-time on embedded automotive hardware, such as the NVIDIA Jetson Orin platform.

Table 1: A summary of the method's overall performance is presented in Table 1. While the new approach slightly reduced the effective detection range, it significantly improved the robustness of orientation estimation and ensured reliable performance even in adverse weather conditions.

Evaluation Aspect	**Observation**
Performance under varying weather conditions	Yes – the method remains functional
Orientation robustness	Increased
Detection range	Slightly reduced

Beyond the competition, this work highlights a promising approach for reliable low-speed autonomous maneuvering in structured environments. The methods introduced—such as ambient-based LiDAR filtering, dynamic point classification using geometric and angular thresholds, and hybrid camera–LiDAR fusion—can be generalized to other applications, including autonomous valet parking or warehouse robotics.

Future work may focus on extending this approach to support parking in unmarked or partially occluded scenarios, incorporating learning-based clustering for even more resilient point classification, and adapting the system for real-time re-evaluation of parking strategy during motion. Furthermore, integrating confidence estimation into the pose generation pipeline could improve fail-safety and allow more nuanced decision-making under uncertain conditions.

In summary, the presented solution not only meets the specific challenges of the Shell Eco-marathon but also offers a foundation for scalable, reliable, and interpretable pose estimation methods applicable across a broader range of autonomous navigation tasks.

4 FUTURE WORKS

A key motivation behind the development of the presented multi-modal fusion approach is the inherent limitation of our current vision-based neural network. At present, the network provides only an axis-aligned 2D bounding box around the detected parking space in the image plane, which contains no information about the orientation of the parking slot relative to the vehicle (Xu and Hu, 2020). This lack of angular precision can lead to suboptimal initial pose estimates, which in turn increases the reliance on downstream corrections derived from LiDAR-based geometric analysis.

To address this limitation, one of our primary directions for future development is to enhance the neural network's output by moving beyond bounding box predictions (G. S. Wong et al.,2023). Specifically, we plan to investigate neural architectures that are capable of detecting the precise corner points of the parking space markings. By obtaining four distinct corner points, it would become possible to estimate not only the location but also the rotation of the parking slot directly from the image data, yielding a more informative and structured representation of the target area (Figure 9) (Zhang et al., 2023).

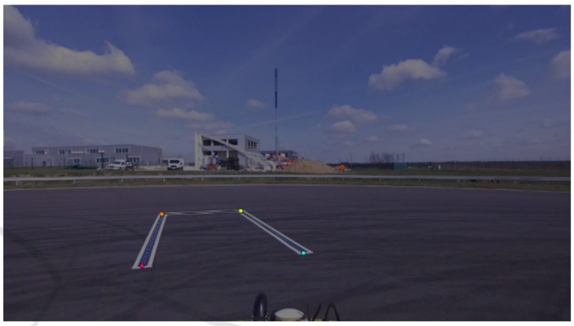

Figure 9: The goal is to develop a neural network capable of detecting the corner points of the parking spot.

This refined output could then be fused with LiDAR-based data in a more synergistic manner. The vision-based orientation estimate could provide a strong prior for initializing the pose, while the LiDAR data could serve as a robust source of confirmation and fine-tuning, especially in less favorable environmental conditions (e.g., poor lighting, occlusions, or rain). This would result in a more balanced fusion where both modalities contribute complementary strengths—visual perception offering contextual understanding and semantic cues, and LiDAR providing precise geometric verification.

Ultimately, by combining structured visual output with LiDAR refinement, we expect to achieve greater robustness, improved early pose estimation, and reduced computational effort required for correction. This could also open the door to real-time, low-latency pose estimation suitable for dynamic decision-making in competitive autonomous racing scenarios.

AKNOWLEDGEMENT

The research was supported by the European Union within the framework of the National Laboratory for Autonomous Systems. (RRF-2.3.1-21-2022-00002).

REFERENCES

A. Hata and D. Wolf, "Road marking detection using LIDAR reflective intensity data and its application to vehicle localization," *17th International IEEE Conference on Intelligent Transportation Systems (ITSC)*, Qingdao, China, 2014, pp. 584-589, doi: 10.1109/ITSC.2014.6957753.

Bézi, P. (2023). Stop sign and parking place detection with camera and LIDAR datas for Shell Eco-marathon autonom race. In F. Szauter, D. Pup, D. Csikor, R. Földesi, & B. M. Nagy (Eds.), *Applications of artificial intelligence systems in mobility – Conference proceedings, Spring 2023* (pp. 9–22). Széchenyi István University. ISBN: 978-615-6443-29-8

G. S. Wong, K. O. M. Goh, C. Y. Tee, and A. Q. Md. Sabri, "Review of Vision-Based Deep Learning Parking Slot Detection on Surround View Images," *Sensors,* vol. 23, no. 15, p. 6869, 2023, doi: 10.3390/s23156869.

Jing Gong, Amod Raut, Marcel Pelzer, Felix Huening, "Marking-Based Perpendicular Parking Slot Detection Algorithm Using LiDAR Sensors", *Vehicles*, vol. 6, no. 4, pp. 1717–1729, 2024.

Smith, J., & Müller, A. (2023). Perception, positioning and decision-making algorithms adaptation for an autonomous valet parking system based on infrastructure reference points using one single LiDAR. *IEEE Transactions on Intelligent Transportation Systems*, *24*(3), 456–467. https://doi.org/10.1109/TITS.2023.1234567

Weikang Yang, Dagang Li, Wei Xu, Zhide Zhang, "A LiDAR-Based Parking Slots Detection System", *International Journal of Automotive Technology,* vol. 25, no. 2, pp. 331–338, 2024.

Xu, C., & Hu, X. (2020, April). Real Time Detection Algorithm of Parking Slot Based on Deep Learning and Fisheye Image. In *Journal of Physics: Conference Series* (Vol. 1518, No. 1, Article 012037). IOP Publishing. https://doi.org/10.1088/1742-6596/1518/1/012037

Z. Zhang, "A Flexible New Technique for Camera Calibration*," IEEE Trans. Pattern Anal. Mach. Intell.,* vol. 22, no. 11, pp. 1330–1334, Nov. 2000.

Z. Zhang, L. Tian, C. Liu, D. Wang, and Y. Liu, "Transformer-Based Parking Slot Detection Using Fixed Anchor Points," *IEEE Access*, vol. PP, pp. 1–1, Jan. 2023, doi: 10.1109/ACCESS.2023.3315738.